Title

Resonant Infrared Multiple Photon Dissociation Spectroscopy of Anionic Nucleotide Monophosphate Clusters

Journal

The Journal of Physical Chemistry B, 119(25)

ISSN

1520-6106 1520-5207

Authors

Ligare, Marshall R
Rijs, Anouk M
Berden, Giel
et al.

Publication Date

2015-06-25

DOI

10.1021/acs.jpcb.5b02222

Peer reviewed

THE JOURNAL OF PHYSICAL CHEMISTRY B

Article

pubs.acs.org/JPCB

Resonant Infrared Multiple Photon Dissociation Spectroscopy of Anionic Nucleotide Monophosphate Clusters

Marshall R. Ligare,[†] Anouk M. Rijs,[‡] Giel Berden,[‡] Martin Kabeláč,[§] Dana Nachtigallova,[∥] Jos Oomens,[‡,⊥,∥] and Mattanjah S. de Vries*[,†]

[†]Department of Chemistry and Biochemistry, University of California Santa Barbara, Santa Barbara, California 93106, United States

[‡]FELIX Facility, Institute for Molecules and Materials, Radboud University Nijmegen, Toernooiveld 7c, 6525 ED Nijmegen, The Netherlands

[§]Faculty of Science, University of South Bohemia, Branišovská 31, 370 05 České Budějovice, Czech Republic

[∥]Institute of Organic Chemistry and Biochemistry, Academy of Sciences of the Czech Republic, 166 10 Prague 6, Czech Republic

[⊥]van 't Hoff Institute for Molecular Sciences, University of Amsterdam, Science Park 904, 1098XH Amsterdam, The Netherlands

Supporting Information

ABSTRACT: We report mid-infrared spectra and potential energy surfaces of four anionic, 2′-deoxynucleotide-5′-monophosphates (dNMPs) and the ionic DNA pairs $[dGMP\text{-}dCMP-H]^{1-}$, $[dAMP\text{-}dTMP-H]^{1-}$ with a total charge of the complex equal to −1. We recorded IR action spectra by resonant IR multiple-photon dissociation (IRMPD) using the FELIX free electron laser. The potential energy surface study employed an on-the-fly molecular dynamics quenching method (MD/Q), using a semiempirical AM1 method, followed by an optimization of the most stable structures using density functional theory. By employing infrared multiple-photon dissociation (IRMPD) spectroscopy in combination with high-level computational methods, we aim at a better understanding of the hydrogen bonding competition between the phosphate moieties and the nucleobases. We find that, unlike in multimer double stranded DNA structures, the hydrogen bonds in these isolated nucleotide pairs are predominantly formed between the phosphate groups. This intermolecular interaction appears to exceed the stabilization energy resulting from base pairing and directs the overall cluster structure and alignment.

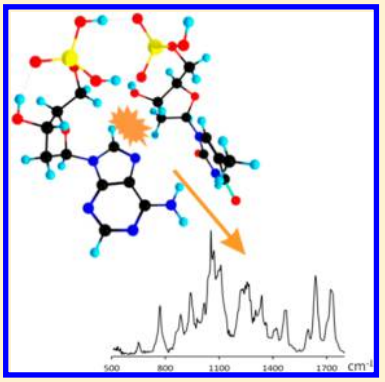

1. INTRODUCTION

A reductionist approach to the study of DNA focuses on the intrinsic properties of its building blocks.[1−3] The nucleotides, as the monomeric form of DNA, have important structural properties that may have played a role in their selection as the alphabet for life as well as affecting the structure/function relationship in biology. By studying nucleotides as isolated molecules in the gas phase, we can gain insight into their intrinsic properties, such as their lowest energy conformational shapes and their preferred hydrogen bonding structures. The nucleotides are large molecules with multiple sites for hydrogen bonding on both the phosphates and the nucleobases. Therefore, multiple intra- and intermolecular interactions govern the overall structures. In order to simplify this complex chemical landscape, it is instructive to remove the solvent and the macromolecular environment in order to chart the detailed competition and interplay of the hydrogen bonding of the phosphates vs the nucleobases.

Hydrogen bonding of mononucleotides in solution has been studied most successfully by proton NMR. The chemical shifts associated with amine hydrogens are sensitive to hydrogen bonding vs base stacking interactions and it was shown that base pair hydrogen bonding competes with base stacking in solution for both single mononucleotides and mixtures.[4] Adenosine nucleotides have also been studied in solution by Infrared[5] and Raman spectroscopy.[6] These pH-dependent studies revealed the frequencies of the anionic phosphate moiety and determined accurate pK_a values for the acidic and basic sites. No conclusions about the hydrogen bonding, either intra or intermolecular, could be drawn due to the large frequency shifts associated with the change in ionic state. Experiments by Thomas and co-workers confirm the existence of the keto and amino tautomers in solution.[7] A comparison of solution phase spectra with solid phase spectra showed strong hydrogen bonding in the crystalline bases uracil, cytosine and adenine but did not yield conclusions about the nucleotides and did not show any interaction between the bases or the phosphates in solution.[7] A later study by Thomas and co-workers examined mixtures of nucleotides, showing no change in the spectrum of pure vs mixed solutions, concluding that only stacked structures were present.[8]

Experiments aimed at studying isolated base pairing interactions typically use nonpolar solvents and substituted nucleosides to minimize hydrogen bonding competition from

Received: March 6, 2015
Revised: May 22, 2015
Published: May 23, 2015

DOI: 10.1021/acs.jpcb.5b02222
J. Phys. Chem. B 2015, 119, 7894−7901

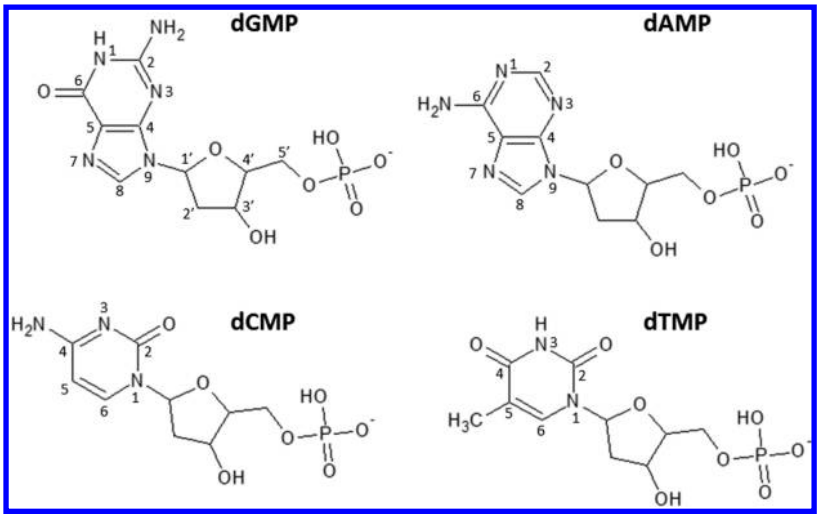

Figure 1. Molecular structures for the four 2′-deoxynucleotide-5′-monophosphate anions.

the solvent and to promote hydrogen bonded base pairing.[9,10] These experiments have revealed that under those conditions many base pairing motifs are possible, for example A-T can form up to four structures that occur with almost equal probability. Such experiments connect gas-phase and solution-phase observations. However, they do not include the phosphate moiety. The phosphate moiety is highly polar and capable of strong hydrogen bonding that should be able to compete with nucleobase bonding in solution as well as in the gas phase.

Figure 1 shows the structures of the four canonical nucleotide ions; these have been previously studied in the gas phase by various mass spectrometry techniques such as collision induced dissociation,[11] H/D exchange,[12] ion mobility[13,14] and IR multiple-photon dissociation (IRMPD) spectroscopy.[15,16] Gas phase structural information using IRMPD spectroscopy has been reported for nucleobase-metal ion clusters,[17,18] protonated nucleobases,[19] and nucleotide ions.[16,20] These past experiments have provided a wealth of information such as, fragmentation pathways, low energy structural conformations and, in the case of ion mobility, energetic barriers between low energy conformations of dinucleotides. All of these experiments have led to the conclusion that the 3′OH stabilizes the negatively charged phosphate group in a strong hydrogen bond that is conserved in all the nucleotides. This interaction holds a fairly large molecule into only a few conformations. Here, we extend these gas-phase spectroscopic studies to the anionic DNA base pairs $[\text{dGMP-dCMP}-\text{H}]^{1-}$, $[\text{dAMP-dTMP}-\text{H}]^{1-}$, where −H denotes a proton missing from the complex. We aim to gain insight in the hydrogen bonding competition between the phosphate moieties and the nucleobases by examining the vibrational frequency differences between the monomers and the clusters.

The structures of biologically relevant forms of DNA become increasingly difficult to determine as the systems become larger in size; more low energy structural isomers may contribute to the spectrum and the presence of more infrared oscillators may result in vibrational congestion. On the other hand, for a successful structural identification the rich vibrational mode information in the mid-IR (500−1800 cm^{-1}) is very useful. This region contains all hydrogen bonding modes through carbonyl, amide, amine and phosphate moieties, facilitating a complete analysis. Therefore, these data can provide structures in greater detail than possible in solution or in the macromolecule. The hope is that the resulting insights can then be extrapolated to include the biological environment.

We perform structural analyses by comparison with a combination of molecular mechanics and ab initio calculations. The role of theory is even more critical here than in the case of neutral species studied by resonance enhanced multiphoton ionization (REMPI) spectroscopy because the experimental data are not isomer specific. At the same time, clusters of the nucleotides pose a challenge for current molecular mechanics/ab initio methods. The large size of the system and the availability of multiple hydrogen bond locations allow for the clusters to adopt many low energy conformations that are quiet diverse in their structure. Therefore, these gas phase data also serve as benchmarks for computational results, allowing optimization of methods and functionals and aiding development of high level theoretical treatments.

2. METHODS

2.1. Computational. To explore the potential energy surfaces, we used a molecular dynamics quenching method, which combines molecular dynamics with a minimization procedure of selected geometries, obtained from the trajectories. We used an on-the-fly molecular dynamics technique, employing a semiempirical AM1 method as an external potential.[21] For the nucleotide pairs we included all possible combinations of charged and neutral nucleotides. Molecular dynamics quenching simulation was performed at 1200 K, which is sufficient to allow crossing over all relevant energy barriers and thus sample the complete potential energy surface. To avoid dissociation, we imposed harmonic restraints on the distances of centers of masses of the molecules in the complexes. The ensemble was sampled by Andersen thermostat with a total simulation time of 1 ns. Every picosecond the structure from the MD trajectory was minimized, with the AM1 method, and stored. The optimized structures were sorted with respect to their conformations and energies. Subsequently, the 50 most stable structures, based on relative Gibbs energies, were further optimized with the B97D[22] density functional and TZVP basis set,[23] employing the density fitting procedure. The optimized structures were subjected to harmonic vibrational analyses and the resulting frequencies were compared without

DOI: 10.1021/acs.jpcb.5b02222
J. Phys. Chem. B 2015, 119, 7894−7901

further scaling with the experimental spectra. The DFT calculations employed the Gaussian09 package.[24]

2.2. Experimental (IRMPD). We obtained infrared action spectra of the anionic nucleotides, 2′-dexoynucleotide-5′-monophosphates and clusters $[dGMP\text{-}dCMP-H]^{1-}$, $[dAMP\text{-}dTMP-H]^{1-}$ from infrared multiple-photon dissociation (IRMPD) using the tunable mid-IR radiation from the free electron laser FELIX (free electron laser for infrared experiments).[25] The ions were generated by electrospray ionization (ESI) and subsequently injected into a 4.7 T actively shielded Fourier transform ion cyclotron resonance mass spectrometer (FT-ICR MS). Irradiation with the free electron laser beam induces fragmentation of the precursor ion to an extent that is dependent on the IR frequency, so that an IR spectrum can be reconstructed from a series of mass spectra recorded at different settings of the IR wavelength. The experimental setup has previously been described in detail.[26,27] The deprotonated nucleotide anions and anionic clusters are generated using a Waters Micromass Z-spray ESI source, which facilitates gentle ionization and vaporization of labile biomolecular species. We chose the −1 rather than −2 cluster ions for this study because of their higher abundance in the mass spectrometer. We used solutions of the mononucleotides of 1 mM in 50:50 H_2O:MeOH. The continuously generated ions are accumulated in a hexapole ion trap, after which they are sent through a quadrupole bender before entering an octopole ion guide that drives the ions into the FT-ICR cell. The anion or anionic cluster of interest is isolated using a SWIFT excitation pulse.[28]

3. RESULTS

3.1. Anionic Monophosphate Nucleotide Monomers. IRMPD spectra of the anionic nucleotides have been reported by Nei et al.[16] The ground state structures and assignments here are in agreement with these earlier results. For the nucleotides all calculated structures except two higher energy structures for $[dGMP-H]^{1-}$ have the 3′OH of the ribose hydrogen bonded to the phosphate. All nucleotides except $[dGMP-H]^{1-}$ are in the anticonfiguration with respect to the nucleobase and the ribose.,[1415] In all cases the sugars line up in the C3′endo conformation with the base and phosphate lying above the plane of the sugar. All experimental and calculated spectra along with the calculated structures are given in Supporting Information. A comparison of the experimental spectra of the monomers and the clusters is shown in Figures 3 and 5 to illustrate the changes in vibrational frequencies due to hydrogen bonding between the monomers

3.2. Anionic Monophosphate Nucleotide Clusters. In each base pair cluster one monophosphate nucleotide is neutral and the other is negatively charged. We obtained 12 low energy calculated structures for each cluster, six where the phosphates on the pyrimidine nucleotides are negatively charged and six where the phosphates on the purine nucleotides are negatively charged. We also considered zwitterionic structures for the neutral nucleotides in the clusters. dGMP has a low energy structure where the N3 position is protonated and the phosphate is deprotonated. For dCMP, dAMP, and dTMP, we found protonation to be too high in energy to be considered.

All of the calculated structures exhibit multiple hydrogen bonds, most of which occur between the phosphate moieties (Supporting Information, Figures SI5 and SI6). The structures calculated here are similar to some of the structures identified in a gas phase ion mobility study of covalently bonded dinucleotides.[13] In nearly all of the structures, the two phosphate moieties are connected by at least one, and in the lowest energy cases two, H-bonds. Only two structures are predicted where the phosphates are H-bonded but the bases are away from each other (Supporting Information Figure SI5, structures **7**, **8**). Our experimental data suggest that this type of structure, if present at all, is in low abundance. The phosphate group can both accept and donate hydrogen bonds with its highly polar P−OH and P═O bonds. The purine and pyrimidine bases can also act as both hydrogen bond donors and acceptors. In all cases except one (Supporting Information Figure SI6, structure **6**), the highly polar phosphates bond to each other with different orientations of the bases relative to the sugar. Although assignment of one single structure is not possible due to spectral congestion and the occurrence of many low energy structures, assignment of a few families of structures is possible. The lowest energy structures for both clusters show an overall spectral shape most similar to the experimental spectra. To simplify the comparison of the monomers and clusters, we will use the frequencies corresponding to the lowest energy structures for the monomers and clusters to illustrate the band shifts seen in the experimental spectra (Figures 3 and 5).

$[dAMP\text{-}dTMP-H]^{1-}$. The computational data suggest that the cluster of neutral dAMP bonded to negatively charged dTMP is more stable than the cluster with the negative charge residing on dAMP. The six lowest energy structures of $[dAMP\text{-}dTMP-H]^{1-}$ fall within a range of 2.1 kcal/mol, all with the charge on the phosphate of dTMP. The lowest energy structure with the charge on dAMP is found at 4.75 kcal/mol. The structures are numbered sequentially in increasing energy (Supporting Information Figure 5)

Figure 2 shows the experimental spectrum with the calculated spectra for comparison. The B97D functional employed predicts the region above 1500 cm^{-1} quite well. Structures 1 and 2 have double hydrogen bonds from dAMP to $[dTMP-H]^{1-}$ between the phosphate groups forming an eight member ring. For all calculated structures, both ribose moieties are in the 3′ *endo* conformation with the exception of dAMP in structure 5 (Supporting Information Figure SI5). Although the experimental spectrum is congested, the clusters are predicted to have intensities for the phosphate, carbonyl and amine modes that are similar to those in the monomers. The carbonyl vibrations on $[dTMP-H]^{-1}$, NH_2 scissor on dAMP and the various phosphate modes are color coded in Figures 2−5. Starting from the high energy region of the spectrum, the yellow bands correspond to carbonyl modes, green to NH_2 symmetric bends, blue to phosphate modes and red to both C−O stretches on the ribose and phosphate modes. The frequency assignments are given in Supporting Information Table SI5. The two lowest energy structures fit the experimental spectrum best considering these modes.

The two monomer spectra are plotted with the cluster spectrum in Figure 3. The carbonyl modes of the $[dTMP-H]^{-1}$ monomer are calculated to be only 15 cm^{-1} apart, however they are split by about twice as much in the cluster. The experimental spectrum shows some broadening of the unresolved carbonyl peaks as well as a blue shift of these vibrations compared to the monomer spectrum. This shift is consistent with the calculated frequencies of structures 1, 2, 4, 5, and 6 of $[dAMP\text{-}dTMP-H]^{1-}$, where the planes of the bases are closer to perpendicular rather than parallel. In structure 3, the only stacked type conformation with the base planes

DOI: 10.1021/acs.jpcb.5b02222
J. Phys. Chem. B 2015, 119, 7894−7901

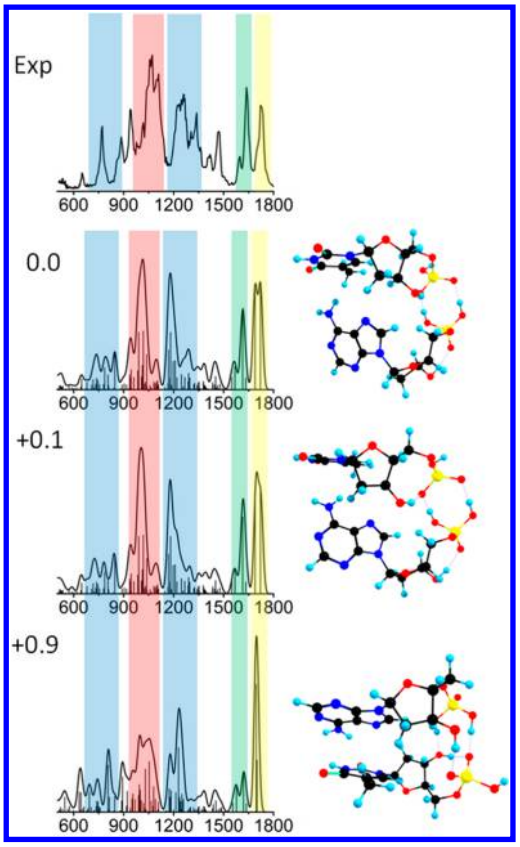

Figure 2. Experimental spectrum of $[dAMP\text{-}dTMP-H]^{1-}$ plotted with the three lowest energy calculated spectra. ΔG energies are given in kcal/mol and are relative to the minimum energy structure.

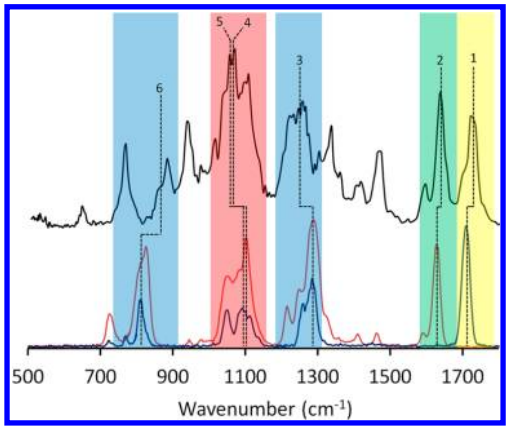

Figure 3. (Black) Experimental spectrum of $[dAMP\text{-}dTMP-H]^{1-}$. (Red) Experimental spectrum of $[dAMP-H]^{1-}$. (Blue) Experimental spectrum of $[dTMP-H]^{1-}$. Dotted lines illustrate the frequency shifts between the lowest energy structures of the monomers and clusters.

oriented parallel to each other, the symmetric and *anti*-symmetric carbonyl stretch modes are predicted to be much more intense and only 5 cm^{-1} apart giving a narrower carbonyl peak than seen experimentally. The NH_2 scissor mode is more intense in the experimental spectrum than predicted in any of the computed spectra, but structures 1 and 2 provide the closest match to the observed intensity and frequency of these modes.

The experimental dissociation yield is much higher for the noncovalently bound clusters than for the monomers. Therefore, the spectral region from 1000 to 1300 cm^{-1} was collected at half the laser power of the rest of the spectrum to avoid saturation. The phosphate stretches have larger transition dipole moments and thus lower laser power is required over this range to fragment the clusters. Furthermore, the clusters are held together by H-bonds rather than by covalent bonds so a smaller number of IR photons is required to reach fragmentation for the clusters than for the monomers. The modes predicted in this region with high intensity are the O−P−O asymmetric and P═O stretches on $[dTMP-H]^{-1}$ and dAMP, respectively and are assigned to the experimental peak centered at 1247 cm^{-1}. In the cluster, only $[dTMP-H]^{-1}$ has an O−P−O asymmetric stretch because dAMP is neutral. The asymmetric stretch on dTMP is predicted to be at 1181 cm^{-1} and the P═O stretch on dAMP at 1168 cm^{-1}. A red shift of 63 cm^{-1} is calculated for the O−P−O asym stretch. The experiment shows a 38 cm^{-1} a red shift between the monomer (1285 cm^{-1}) and the cluster (1247 cm^{-1}), illustrated by dotted line #3 in Figure 3. All of the cluster phosphate stretches appear to the blue of the calculated frequencies analogous to the shifts in the monophosphates. Scuderi and co-workers have also reported phosphate stretches and bends to the blue of the calculated frequencies.[15] We tentatively assign the experimental peak centered at 1245 cm^{-1} to these two modes. The most intense peak in the spectrum corresponds to both C5′−OPO_3 stretches separated by 27 cm^{-1} calculated at 991 and 1018 cm^{-1}. Experimentally these peaks are at 1072 and 1110 cm^{-1}, respectively. These peaks are unresolved and quite broad at the base suggesting that other modes are also contributing. Structures **3** and **4** are relatively low in energy but do not show the same relative intensities for these sugar and phosphate modes. Therefore, it is difficult to determine whether or not they contribute to the spectrum. A direct comparison between the monomer and the cluster spectra in the region, marked by the red band in Figure 3, is difficult due to coupling of many of the modes, so only the two C5′-OPO_3 modes mentioned above are compared in this region: These modes are marked by the dotted lines labeled 4 and 5 for dAMP and dTMP respectively in Figure 3. For other modes assigned to these experimental peaks see Supporting Information, Tables SI1, SI2, and SI5. For the lowest energy band marked in blue only the P−OH stretch on dTMP is compared between the monomer and cluster which is predicted to blue shift ∼50 cm^{-1} as shown by the dotted line 5. The other modes in the cluster spectrum below 1400 cm^{-1} with no assignment are new modes arising from the changes in symmetry in the neutral dAMP portion of the cluster but are assigned to the cluster spectrum in Supporting Information, Table SI5.

$[dGMP\text{-}dCMP-H]^{1-}$. Analogously to structures 1−5 of $[dAMP\text{-}dTMP - H]^{1-}$, structure 1 of $[dGMP\text{-}dCMP-H]^{1-}$ is charged on the pyrimidine nucleotide. As shown in Figure 4, the experimentally observed C═O and NH_2 modes of $[dGMP\text{-}dCMP-H]^{1-}$ are reproduced quite well by structure 1. The peak at 1703 cm^{-1} matches the C═O stretch at 1705 cm^{-1} resulting from dGMP hydrogen bonded to dCMP. In the monomer the carbonyl is unbound and appears at 1717 cm^{-1} while predicted at 1719 cm^{-1}. For the cluster, the calculation predicts that the carbonyl of dGMP is H-bonded to the NH_2 of $[dCMP-H]^{-}$ and therefore this mode shifts by 12 cm^{-1} to the red. This is in close agreement with the 13 cm^{-1} shift observed experimentally, from 1717 to 1704 cm^{-1}, shown in Figure 5 assignment 1. The carbonyl stretch of $[dCMP-H]^{1-}$ is present in two modes of the cluster. It is H-bonded to NH_2 of guanine producing a red shift in both modes relative to the monomer.

DOI: 10.1021/acs.jpcb.5b02222
J. Phys. Chem. B 2015, 119, 7894−7901

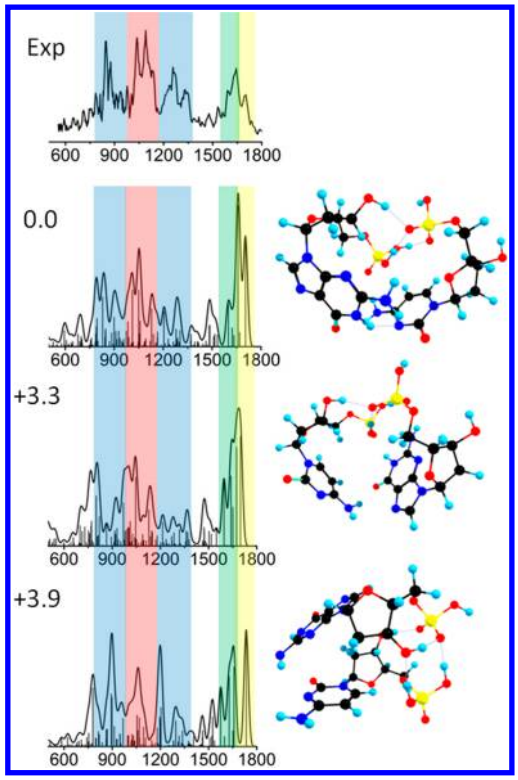

Figure 4. Experimental spectrum of $[dGMP\text{-}dCMP-H]^{1-}$ plotted with the three lowest energy calculated spectra. ΔG energies are given in kcal/mol and are relative to the minimum energy structure.

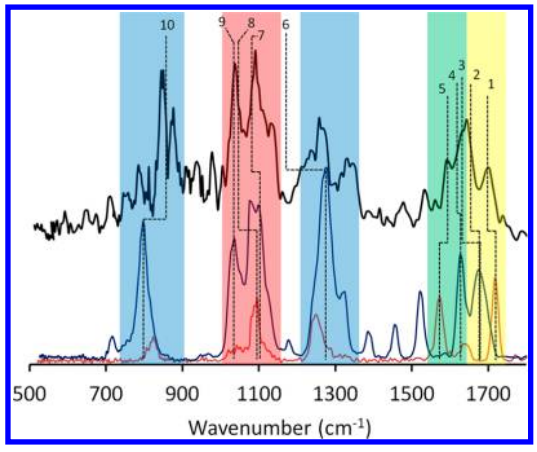

Figure 5. (Black) Experimental spectrum of $[dGMP\text{-}dCMP-H]^{1-}$. (Red) Experimental spectrum of $[GMP-H]^{1-}$. (Blue) Experimental spectrum of $[dCMP-H]^{1-}$. Dotted lines illustrate the frequency shifts between the lowest energy structures of the monomers and clusters.

The higher energy of the two is predicted to be the more intense and shifted by 15 cm^{-1}. (assignment 2). The lower energy frequency is shifted by 50 cm^{-1} and has one-third the intensity of the former (assignment 3) The two red-shifted carbonyls of $[dCMP-H]^{1-}$ predicted in the cluster are on either side of largest peak in the experimental spectrum with the higher energy mode having the largest intensity of all the calculated modes for structure 1. This spectral feature most clearly distinguishes the two lowest energy structures in the region above 1600 cm^{-1} and suggests that the lowest energy structure, **1**, of $[dGMP\text{-}dCMP-H]^{1-}$, is the largest contributor to the experimental spectrum. Overall the phosphate modes are calculated to the red, as was the case for $[dAMP\text{-}dTMP-H]^{1-}$, but considering these modes, $[dGMP\text{-}dCMP-H]^{1-}$ structure 1 is the one most similar to the experiment. The other, higher energy, structures shown in Supporting Information Figure SI6 do not match the experimental spectrum in either the phosphate or carbonyl/amine regions. Similar spectral shifts assigned for the phosphate and C5′-OPO stretches in $[dAMP\text{-}dTMP-H]^{1-}$ are assigned for $[dGMP\text{-}dCMP-H]^{1-}$ (6−10). One exception is the 100 cm^{-1} red shift predicted for the asymmetric O−P−O stretch, assignment 6, which does not fit any shifts seen in the experimental spectrum.

$[dGMP\text{-}dCMP-H]^{1-}$ Cluster with Zwitterionic dGMP. The calculations also predict two low energy zwitterionic structures. In that case the N3 position on guanine is protonated and the phosphate is deprotonated leaving an overall neutral molecule that can bind to the negatively charged $[dCMP-H]^{1-}$ giving a negatively charged cluster. The spectrum for these structures is given in Supporting Information Figure 7 along with the experimental spectrum. A dominant feature of the spectrum comes from the N−H bends in the 1700−1720 cm^{-1} range which involves an N3H and N1H coupled symmetric in-plane bend and both are H-bonded to either their own phosphate or the other nucleotide's phosphate. Furthermore, the N1H stretch is red-shifted into the 1800 cm^{-1} and is predicted to have an intensity nearly three times that of any other mode below 2000 cm^{-1}. Since the experimental spectrum is limited to 1800 cm^{-1} it is difficult to tell if these structures are present. If the prediction of the intensity and location of this absorbance is within about 20 cm^{-1}, we would expect to see a large increase in fragmentation at the 1800 cm^{-1} edge of the experimental spectrum, which we did not observe. All phosphate modes are predicted to the blue of the experimental range while all other organic modes are predicted accurately or slightly to the red if hydrogen bonded. This would suggest that these strongly hydrogen bonded organic modes should be just inside of the experimental range but the overall experimental spectrum does not seem to exhibit any of the major modes predicted for these structures. Two new modes are predicted in the region between 1500 and 1600 cm^{-1} from a coupled in-plane asymmetric bend of the two N−H bonds. This produces the large change in the calculated spectrum for this region, which also does not match the experiment. On the basis of these observations, we conclude that zwitterionic structures are not formed in the experiment.

4. DISCUSSION

The DFT calculations predict the monomer deoxynucleotide vibrational frequencies quite well. Although the phosphate symmetric and asymmetric stretches are observed at about 50 cm^{-1} to the blue of those calculated and about 100 cm^{-1} to the blue for the P−OH stretches, the assignments for these modes can be considered secure based on their high intensities and on comparison with other IR experiments probing phosphates[5,29] and organophosphates.[30,31] Scuderi and co-workers and Rodgers and co-workers reported similar findings for the cyclic 3′,5′-adenosine monophosphate anion and 2′-deoxynucleotide-5′-monophosphate anions respectively using resonant IRMPD.[15,16] Since the carbonyl and amine frequencies for nearly all the monomer structures match the experimental spectra, the structuraly most diagnostic frequencies come from the phosphate. For $[dAMP-H]^{1-}$ and $[dGMP-H]^{1-}$ we can tentatively assign the calculated lowest energy structures to be dominant but for $[dCMP-H]^{1-}$ the four lowest energy

DOI: 10.1021/acs.jpcb.5b02222
J. Phys. Chem. B 2015, 119, 7894−7901

structures are so similar and close in energy that they all may be present. For $[dTMP-H]^-$ the two lowest energy structures appear to be present in the experiment.

For the clusters, all calculated structures up to 5.5 kcal/mol show a phosphate-phosphate interaction, but the bases may occur as either parallel or perpendicular. At higher energies, for $[dGMP\text{-}dCMP-H]^{1-}$ at 5.6 kcal/mol the computation predicts a structure in which the phosphates are bonded to the nucleobases and not to each other. This is the only example of this motif. This observation is consistent with the prediction that (1) this cluster is capable of more hydrogen bonds and (2) the $[dGMP-H]^{1-}$ monomer is in the *syn*-conformation rather than the *anti*-conformation, giving the nucleotide the ability to be low in energy as a curled rather than extended structure. This propensity for the *syn*-conformation rather than *anti*-conformation seems to be mostly conserved in the clusters and consequently a larger diversity of structures appears in the calculations, albeit with a much higher energy gap from the lowest energy structure. Even with these differences in the base pair clusters, the third lowest energy (stacked type) structures are remarkably similar and show a change in the 3′OH hydrogen bond from stabilizing its own phosphate to bonding with the adjacent nucleotide. The overall structure of the base, ribose and phosphate seems to drive this change in interaction.

The $[dGMP\text{-}dCMP-H]^{1-}$ cluster can form three hydrogen bonds between the nucleobases as opposed to $[dAMP\text{-}dTMP-H]^{1-}$ which can form only two hydrogen bonds. This extra H-bonding competes favorably with the bonding between the phosphate groups and thus changes the lowest energy structures from nonbonding bases in $[dAMP\text{-}dTMP-H]^{1-}$ to the stacked motifs in $[dGMP\text{-}dCMP-H]^{1-}$. A major difference appears between $[dGMP\text{-}dCMP-H]^{1-}$ and $[dAMP\text{-}dTMP-H]^{1-}$ for the preference of the charge location. While $[dAMP\text{-}dTMP-H]^{1-}$ has the six lowest energy structures with the charge on dTMP, the lowest energy for $[dGMP\text{-}dCMP-H]^{1-}$ has its charge on dCMP and for the next two low energy structures the charge is on dGMP. There is a much larger energy gap between structures **1** and **2**, giving a predicted abundance of above 99% for the lowest energy structure $[dGMP\text{-}dCMP-H]^{1-}$ #1.

The structural differences seen in the mononucleotides up to ∼7 kcal/mol were small and only include the location and direction of the hydrogen bonded to the phosphate and the orientation of the phosphate relative to the ribose. Features that are conserved in dAMP, dTMP and dCMP are (i) the perpendicular orientations of the base vs the sugar and (ii) the anti configuration of the base relative to the sugar and the phosphate, both of which are structural features in DNA. Perhaps the most important feature is the stabilization of the phosphate by the 3′OH of the ribose, predicted in 22 of the 24 monomer structures and conserved in many of the cluster structures.

In the clusters, the phosphates are bonded to each other in 23 of the 24 structures showing the strength of the phosphate hydrogen bonding. This strong interaction is of *importance to theories of prebiotic chemistry* because autopolymerization of nucleotides is predicted to be one of the ways in which DNA or RNA may have been synthesized prior to polymerase enzymes.,[32,33] Although these structures may not predict the ability of the phosphates to autopolymerize they are characterized by a significant H-bonding interaction.

An intriguing aspect is the change that occurs between the lowest energy structures and the stacked type structures. In both clusters pairs the third lowest energy structure is stacked (Figure 6). In that case the hydrogen bonding preference of the

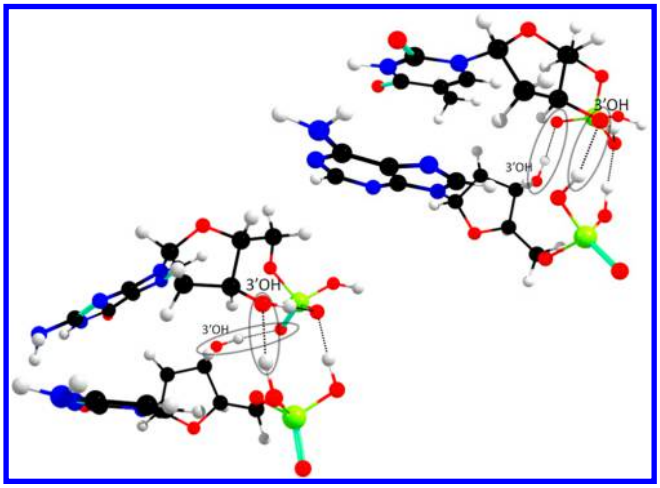

Figure 6. Molecular structures of the third lowest energy structures for both clusters. (Top/Right) $[dAMP\text{-}dTMP-H]^{1-}$. (Bottom/Left) $[dGMP\text{-}dCMP-H]^{1-}$.

3′OH changes from its own phosphate to the phosphate on the adjacent nucleotide. DNA polymerase has one of the highest fidelity rates in biopolymerization. For fast polymerization the complex must be able to take in the monomer quickly, make small conformational changes, and add the monomer to the chain. The gas phase cluster structures derived from this study are very similar to structures calculated for the deoxynucleotide triphosphates (dNTP) bonding in the active site of DNA polymerase[34,35] and in X-ray crystal structures from permanently bonded or trapped analogues to dNTPs.[36]

This finding suggests that in the gas phase, free of solvent effects, the hydrogen bonding of the phosphates and the interaction of the bases directs the alignment of the nucleotides. It appears that base stacking changes the interaction of the 3′OH from its own phosphate to the adjacent phosphate. This structural motif is analogous to structures optimized for quick incorporation into DNA polymerase in the biological environment. Furthermore, the stacked structure of $[dGMP\text{-}dCMP-H]^{1-}$ is the only one in which the nucleotides adopt conformations similar to those of dAMP, dCMP, and dTMP monomers in the biological environment. Thus, it appears that when the bases stack, the 3′OH hydrogen bonding to the adjacent nucleotide creates the biologically relevant monomer structures within the clusters which out competes the third hydrogen bond of the lowest energy $[dGMP\text{-}dCMP-H]^{1-}$ cluster.

■ ASSOCIATED CONTENT

Supporting Information

All experimental and calculated spectra along with the calculated structures of the monomers as well as frequency assignments for monomers and clusters. The Supporting Information is available free of charge on the ACS Publications website at DOI: 10.1021/acs.jpcb.5b02222.

■ AUTHOR INFORMATION

Corresponding Author

*(M.S.d.V.) E-mail: devries@chem.ucsb.edu. Telephone: +1 (805) 893-5921.

DOI: 10.1021/acs.jpcb.5b02222
J. Phys. Chem. B 2015, 119, 7894−7901

Notes

The authors declare no competing financial interest.

■ ACKNOWLEDGMENTS

This material is based upon work supported by the National Science Foundation under CHE-1301305 and by NASA under Grant No. NNX12AG77G. This work is part of the research programme of the Stichting voor Fundamenteel Onderzoek der Materie (FOM), which is financially supported by the Nederlandse Organisatie voor Wetenschappelijk Onderzoek (NWO). We gratefully thank the FELIX staff for their skillful experimental support. D.N. acknowledges the funding of the Grant Agency of the Czech Republic (P208/12/1318). The research at IOCB was a part of the project RVO:61388963.

■ REFERENCES

(1) De Vries, M. S.; Hobza, P. Gas-Phase Spectroscopy of Biomolecular Building Blocks. *Annu. Rev. Phys. Chem.* **2007**, *58*, 585−612.

(2) Kleinermanns, K.; Nachtigallova, D.; De Vries, M. S. Excited State Dynamics of DNA Bases. *Int. Rev. Phys. Chem.* **2013**, *32* (2), 308−342.

(3) Middleton, C. T.; De La Harpe, K.; Su, C.; Law, Y. K.; Crespo-Hernandez, C. E.; Kohler, B. DNA Excited-State Dynamics: From Single Bases to the Double Helix. *Annu. Rev. Phys. Chem.* **2009**, *60*, 217−239.

(4) Raszka, M.; Kaplan, N. O. Association by Hydrogen-Bonding of Mononucleotides in Aqueous-Solution. *Proc. Natl. Acad. Sci. U.S.A.* **1972**, *69* (8), 2025−&.

(5) Nakanishi, K.; Hashimoto, A.; Pan, T.; Kanou, M.; Kameoka, T. Mid-Infrared Spectroscopic Measurement of Ionic Dissociative Materials in the Metabolic Pathway. *Appl. Spectrosc.* **2003**, *57* (12), 1510−1516.

(6) Rimai, L.; Cole, T.; Parsons, J. L.; Hickmott, J. T.; Carew, E. B. Studies of Raman Spectra of Water Solutions of Adenosine Tri- Di- and Monophosphate and Some Related Compounds. *Biophys. J.* **1969**, *9* (3), 320−&.

(7) Lord, R. C.; Thomas, G. J. Raman Spectral Studies of Nucleic Acids and Related Molecules.I. Ribonucleic Acid Derivatives. *Spectrochim Acta, Part A* **1967**, *A 23* (9), 2551−&.

(8) Lord, R. C.; Thomas, G. J. Raman Studies of Nucleic Acids 0.2. Aqueous Purine and Pyrimidine Mixtures. *Biochim. Biophys. Acta* **1967**, *142* (1), 1.

(9) Yang, M.; Szyc, L.; Rottger, K.; Fidder, H.; Nibbering, E. T. J.; Elsaesser, T.; Temps, F. Dynamics and Couplings of N-H Stretching Excitations of Guanosine-Cytidine Base Pairs in Solution. *J. Phys. Chem. B* **2011**, *115* (18), 5484−5492.

(10) Greve, C.; Preketes, N. K.; Fidder, H.; Costard, R.; Koeppe, B.; Heisler, I. A.; Mukamel, S.; Temps, F.; Nibbering, E. T. J.; Elsaesser, T. N-H Stretching Excitations in Adenosine-Thymidine Base Pairs in Solution: Pair Geometries, Infrared Line Shapes, and Ultrafast Vibrational Dynamics. *J. Phys. Chem. A* **2013**, *117* (3), 594−606.

(11) Rodgers, M. T.; Campbell, S.; Marzluff, E. M.; Beauchamp, J. L. Low-Energy Collision-Induced Dissociation of Deprotonated Dinucleotides - Determination of the Energetically Favored Dissociation Pathways and the Relative Acidities of the Nucleic-Acid Bases. *Int. J. Mass Spectrom. Ion Process* **1994**, *137*, 121−149.

(12) Freitas, M. A.; Marshall, A. G. Gas Phase RNA and DNA Ions 2. Conformational Dependence of the Gas-Phase H/D Exchange of Nucleotide-5′-Monophosphates. *J. Am. Soc. Mass Spectrom.* **2001**, *12* (7), 780−785.

(13) Gidden, J.; Bowers, M. T. Gas-Phase Conformational and Energetic Properties of Deprotonated Dinucleotides. *Eur. Phys. J. D* **2002**, *20* (3), 409−419.

(14) Gidden, J.; Bowers, M. T. Gas-Phase Conformations of Deprotonated and Protonated Mononucleotides Determined by Ion Mobility and Theoretical Modeling. *J. Phys. Chem. B* **2003**, *107* (46), 12829−12837.

(15) Chiavarino, B.; Crestoni, M. E.; Fornarini, S.; Lanucara, F.; Lemaire, J.; Maitre, P.; Scuderib, D. Infrared Spectroscopy of Isolated Nucleotides 1. the Cyclic 3′,5′-Adenosine Monophosphate Anion. *Int. J. Mass Spectrom.* **2008**, *270* (3), 111−117.

(16) Nei, Y. W.; Hallowita, N.; Steill, J. D.; Oomens, J.; Rodgers, M. T. Infrared Multiple Photon Dissociation Action Spectroscopy of Deprotonated DNA Mononucleotides: Gas-Phase Conformations and Energetics. *J. Phys. Chem. A* **2013**, *117* (6), 1319−1335.

(17) Nei, Y. W.; Akinyemi, T. E.; Kaczan, C. M.; Steill, J. D.; Berden, G.; Oomens, J.; Rodgers, M. T. Infrared Multiple Photon Dissociation Action Spectroscopy of Sodiated Uracil and Thiouracils: Effects of Thioketo-Substitution On Gas-Phase Conformation. *Int. J. Mass Spectrom.* **2011**, *308* (2−3), 191−202.

(18) Salpin, J. Y.; Gamiette, L.; Tortajada, J.; Besson, T.; Maitre, P. Structure of Pb^{2+}/Dcmp and Pb^{2+}/Cmp Complexes As Characterized by Tandem Mass Spectrometry and Irmpd Spectroscopy. *Int. J. Mass Spectrom.* **2011**, *304* (2−3), 154−164.

(19) Nei, Y. W.; Akinyemi, T. E.; Steill, J. D.; Oomens, J.; Rodgers, M. T. Infrared Multiple Photon Dissociation Action Spectroscopy of Protonated Uracil and Thiouracils: Effects of Thioketo-Substitution On Gas-Phase Conformation. *Int. J. Mass Spectrom.* **2010**, *297* (1−3), 139−151.

(20) Schinle, F.; Crider, P. E.; Vonderach, M.; Weis, P.; Hampe, O.; Kappes, M. M. Spectroscopic and Theoretical Investigations of Adenosine 5′-Diphosphate and Adenosine 5 ′-Triphosphate Dianions in the Gas Phase. *Phys. Chem. Chem. Phys.* **2013**, *15* (18), 6640−6650.

(21) Dewar, M. J. S.; Zoebisch, E. G.; Healy, E. F.; Stewart, J. J. P. the Development and Use of Quantum-Mechanical Molecular-Models 0.76. Am1 - A New General-Purpose Quantum-Mechanical Molecular-Model. *J. Am. Chem. Soc.* **1985**, *107* (13), 3902−3909.

(22) Grimme, S. Semiempirical Gga-Type Density Functional Constructed with a Long-Range Dispersion Correction. *J. Comput. Chem.* **2006**, *27* (15), 1787−1799.

(23) Schafer, A.; Huber, C.; Ahlrichs, R. Fully Optimized Contracted Gaussian-Basis Sets of Triple Zeta Valence Quality for Atoms Li to Kr. *J. Chem. Phys.* **1994**, *100* (8), 5829−5835.

(24) Frisch, M. J.; G. W. T, Schlegel, H.B.; Scuseria, G. E.; Robb, M. A.; Cheeseman, J. R.; Scalmani, G.; Barone, V.; Mennucci, B.; Petersson, G. A.; Nakatsuji, H.; M et al., Gaussian 09. Gaussian Inc.: Wallingford CT, 2009.

(25) Oepts, D.; Van Der Meer, A. F. G.; Van Amersfoort, P. W. the Free-Electron-Laser User Facility Felix. *Infrared Phys. Technol.* **1995**, *36* (1), 297−308.

(26) Valle, J. J.; Eyler, J. R.; Oomens, J.; Moore, D. T.; Van Der Meer, A. F. G.; Von Helden, G.; Meijer, G.; Hendrickson, C. L.; Marshall, A. G.; Blakney, G. T. Free Electron Laser-Fourier Transform Ion Cyclotron Resonance Mass Spectrometry Facility for Obtaining Infrared Multiphoton Dissociation Spectra of Gaseous Ions. *Rev. Sci. Instrum.* **2005**, *76*, 2.

(27) Polfer, N. C.; Oomens, J. Reaction Products in Mass Spectrometry Elucidated with Infrared Spectroscopy. *Phys. Chem. Chem. Phys.* **2007**, *9* (29), 3804−3817.

(28) Marshall, A. G.; L. W, T. C.; Ricca, T. L. Tailored Excitation for Fourier Transform Ion Cyclotron Mass Spectrometry. *J. Am. Chem. Soc.* **1985**, 7893−7897.

(29) Klahn, M.; Mathias, G.; Kotting, C.; Nonella, M.; Schlitter, J.; Gerwert, K.; Tavan, P. Ir Spectra of Phosphate Ions in Aqueous Solution: Predictions of A Dft/Mm Approach Compared with Observations. *J. Phys. Chem. A* **2004**, *108* (29), 6186−6194.

(30) Fales, B. S.; Fujamade, N. O.; Nei, Y. W.; Oomens, J.; Rodgers, M. T. Infrared Multiple Photon Dissociation Action Spectroscopy and Theoretical Studies of Diethyl Phosphate Complexes: Effects of Protonation and Sodium Cationization On Structure. *J. Am. Soc. Mass. Spectrom.* **2011**, *22* (1), 81−92.

(31) Wang, L. J.; Yang, L. G.; Keiderling, T. A. Vibrational Circular-Dichroism of A-Form, B-Form, and Z-Form Nucleic-Acids in the Po(2)(−)Stretching Region. *Biophys. J.* **1994**, *67* (6), 2460−2467.

DOI: 10.1021/acs.jpcb.5b02222
J. Phys. Chem. B 2015, 119, 7894−7901

(32) Franchi, M.; Gallori, E. Origin, Persistence and Biological Activity of Genetic Material in Prebiotic Habitats. *Orig. Life Evol. Biosph.* **2004**, *34* (1−2), 133−141.
(33) Cafferty, B. J.; Gallego, I.; Chen, M. C.; Farley, K. I.; Eritja, R.; Hud, N. V. Efficient Self-Assembly in Water of Long Noncovalent Polymers by Nucleobase Analogues. *J. Am. Chem. Soc.* **2013**, *135* (7), 2447−2450.
(34) Pelletier, H.; Sawaya, M. R.; Kumar, A.; Wilson, S. H.; Kraut, J. Structures of Ternary Complexes of Rat DNA-Polymerase-Beta, A DNA Template-Primer, and Ddctp. *Science* **1994**, *264* (5167), 1891−1903.
(35) Pelletier, H.; Sawaya, M. R.; Wolfle, W.; Wilson, S. H.; Kraut, J. Crystal Structures of Human DNA Polymerase Beta Complexed with DNA: Implications for Catalytic Mechanism, Processivity, and Fidelity. *Biochemistry* **1996**, *35* (39), 12742−12761.
(36) Arndt, J. W.; Gong, W. M.; Zhong, X. J.; Showalter, A. K.; Liu, J.; Dunlap, C. A.; Lin, Z.; Paxson, C.; Tsai, M. D.; Chan, M. K. Insight Into the Catalytic Mechanism of DNA Polymerase Beta: Structures of Intermediate Complexes. *Biochemistry* **2001**, *40* (18), 5368−5375.

DOI: 10.1021/acs.jpcb.5b02222
J. Phys. Chem. B 2015, 119, 7894−7901